Effect of the level of the addition of $Pb(Y_{0.5}Nb_{0.5})O_3$ on the structure, microstructure and ferroelectric properties of PZT(53/47)

A. BEITOLLAHI*, M. ABEDINI
Ceramic Division, Department of Metallurgy and Materials Engineering, Iran University of Science and Technology (IUST), Narmak, Tehran, Iran
E-mail: beitolla@iust.ac.ir

Published online: 21 April 2006

In this work an attempt is made to study $[Pb(Zr_{0.53}Ti_{0.47}O_3)O_3]_{1-X}$-$[Pb(Y_{0.5}Nb_{0.5})O_3]_X$ system with $x = 0.0125$, 0.025, 0.05, 0.075 and 0.1. It was shown that there is limited solid solubility (2.5 mol%) of $Pb(Y_{0.5}Nb_{0.5})O_3$ (PYN) in PZT (53/47). The substitution of PYN gave rise to the reduction of the volume of PZT's unit cell. For the samples doped above this level of PYN, an extra phase comprising of Y^{3+}, Zr^{4+} and Ti^{4+} cations were detected based on EDS-SEM and XRD analysis and also a structural shift towards a rhombohedral phase was noticed for the main PZT phase. Further, the addition of PYN up to 2.5 mol% was seen to increase the room temperature relative permittivity and d_{33} parameter. However, these parameters declined for the samples substituted with more than 2.5 mol% PYN due to the formation of non ferroelectric extra phase.

1. Introduction

Lead zirconate titanate $Pb(Zr_{1-X}Ti_X)O_3$, PZT, solid solution system with the compositions near the morphotropic phase boundary ($x = 0.47$) is well recognized for its very interesting and desirable piezoelectric properties [1–4] making it a very attractive candidate for a wide range of electronic applications. Since its discovery in order to enhance its piezoelectric properties both the effects of different processing conditions [5–9] and substitutions of various dopants [1, 10–14] of different ionic sizes and valences have been studied. Beitollahi and Khezri [15] have already reported the effect of the addition of Y_2O_3 on the structure, microstructure and piezoelectric properties of this compound. Following the previous work [15] we in this work report the effect of the addition of $Pb(Y_{0.5}Nb_{0.5})O_3$, on various properties of $PbZr_{0.53}Ti_{0.47}O_3$(PZT 53/47) system.

2. Experimentals

Conventional ceramic route was used for the fabrication of the samples studied in this work. The starting raw materials used were PbO(>99.6% purity) ZrO_2(>99.5% purity) TiO_2(>99.6% purity) Nb_2O_5(>99.8% purity) and $Y(NO_3)_3 \cdot 6H_2O$ (>99.9% purity). For the synthesis of PZT(53/47) compound initially the raw material were accurately weighed according to the stoichiometry and then were wet mixed for 6 h in a polyethylene jar with yttrium doped tetragonal zirconia (YTZ) balls in deionized water. The obtained slurry was later dried in oven at 80°C for 8 h. The mixture was then pulverized in an agate mortar and pestle and subsequently passed through a 100 μm sieve in order to break large agglomerates. The obtained powder was later calcined at 850°C for 2 h in a pure alumina boat covered and sealed by an alumina plate. The calcined powder was again wet milled for 12 h and oven dried. The PYN compound was also prepared separately with ceramic route. In this respect, appropriate amounts of Nb_2O_5 oxide were wet mixed with $Y(NO_3)_3 \cdot 6H_2O$ in deionized water and subsequently dried overnight at 80°C. The obtained powder was then calcined at 1350°C for 2 h and subsequently wet milled for 12 h with appropriate amounts of PbO. The obtained product was again calcined at 850°C for 2 h. X-ray diffraction (XRD) analysis of the obtained powder confirmed the formation of single phase PYN compound. For the preparation of the final powder sample batches these two separately prepared compounds i.e. PZT(53/47) and PYN were wet milled for

*Author to whom all correspondence should be addressed.
0022-2461
DOI: 10.1007/s10853-006-6297-1

8 h in deionized water with the below mentioned molar ratios:

1. PZT (98.75 mol%) + PYN (1.25 mol%)
2. PZT (97.5 mol%) + PYN (2.5 mol%)
3. PZT (95 mol%) + PYN (5 mol%)
4. PZT (92.5 mol%) + PYN (7.5 mol%)
5. PZT (90 mol%) + PYN (10 mol%)
6. PZT (100 mol%)

A 0.5 wt% polyvinyl Alcohol (PVA) binder solution was later also added before the last two hours of this final milling. The mean particle size of the calcined-ball milled powder determined by a Micromeritics particle size analyzer was in the range of 0.3–0.5 μm. The milled slurries of the above samples were then dried and disc shaped samples were subsequently made at a pressure of 2 ton cm^{-2}. The pressed pellets were dried at 70°C for 12 h. In order to remove the organic binder, the samples were decarbonized at 500°C for 4 h in air atmosphere. Finally, these samples were sintered at 1270°C for 2 h with the double crucible arrangement with a ($PbZrO_3$ + 2% PbO) atmosphere powder. Flat and polished samples were prepared before gold sputtering of the sample faces with a sputter coater. Poling of the samples before piezoelectric measurements was done at an electric field of 3 MV/m in silicone oil at 100°C. For XRD characterization a Fe-K_α radiation was used and Si powder was also used as internal standard. Morphology studies and grain size measurement (line-intercept method) and chemical analysis were performed using a Leica Cambridge S360 model scanning electron microscope (SEM) with attached EDS-system. For room temperature dielectric measurements at 1 kHz an automatic HP-4270A capacitance bridge was utilized. For the evaluation of the d_{33} parameter, a Berlincourt piezo-d_{33} meter was used. The magnitudes of g_{33} parameters were also calculated using the measured values of d_{33} and permittivity values. Electrical resistivity was also measured using a 617 Keithley electrometer. The fired densities of the samples were determined by the Archimedes method in water.

3. Results

3.1. Density measurements

Fig. 1 demonstrates the variation of the bulk densities of the sintered samples with the level of PYN concentration. As shown in this figure, a rising trend was observed for the magnitudes of the bulk densities of the samples doped with up to 2.5 mol% PYN. However, doping PZT samples beyond this level gave rise to an appreciable decrease of the measured sintered bulk densities.

3.2. XRD results

Fig. 2 displays XRD multiplot pattern for the whole series of the samples studied in this work. For the pure PZT samples all of the diffraction lines corresponding to the single phase tetragonal PZT(53/47) could be indexed for this sample. However, for the PZT samples doped with more than 2.5 mol% PYN, the observed splittings for the [002] and [211] reflections were remarkably reduced and disappeared implying a structural shift towards rhombohedral phase [16]. Further, upon the addition of PYN to the PZT compounds all of the diffraction peaks widen and for the samples with more than 5 mole% PYN some other extra peaks were also detected. The extra peaks observed could be closely matched with those of JCPDS-XRD data of $Zr_{0.82}Y_{0.18}O_{0.91}$ phase. Table I also summarizes the tetragonal lattice parameters of the undoped PZT, as well as 1.25, 2.5 mol% PYN added samples. As is clear from this table, the addition of PYN up to 2.5 mol% has given rise to the decrease of lattice parameters.

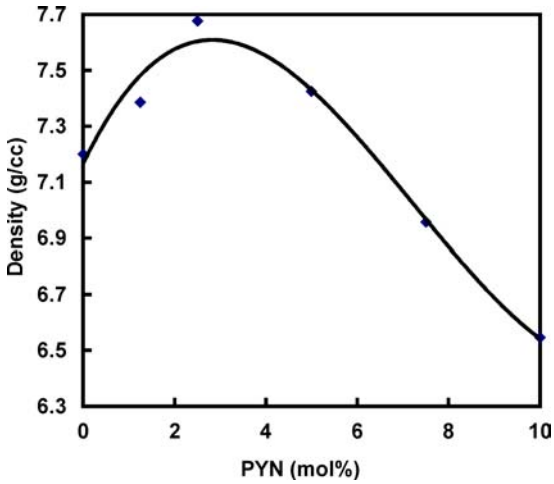

Figure 1 Variation of sintered density versus $Pb(Y_{0.5}Nb_{0.5})O_3$ (PYN) concentration.

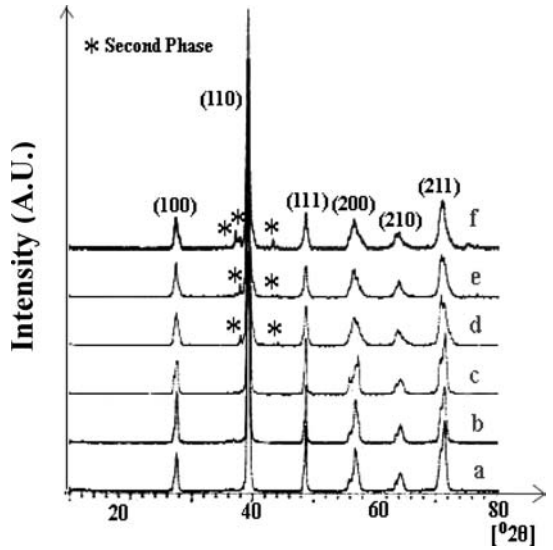

Figure 2 XRD multiplot of the whole series of the system studied in this work. In this figure the letters (a), (b), (c), (d), (e) and (f) correspond to the samples with $x = 0.0$, 0.0125, 0.025, 0.05, 0.075 and 0.1, respectively.

TABLE I Lattice parameters of the pure and $Pb(Y_{0.5}Nb_{0.5})O_3$ – doped samples

	Lattice parameters	
Sample	*a* (nm)	*c* (nm)
Undoped PZT	0.4057	0.4193
1.25 mole% doped PZT	0.4041	0.4187
2.5 mole% doped PZT	0.4037	0.4093

3.3. Dielectric and piezoelectric properties

Fig. 3 presents the variation of room temperature (r.t.) relative permittivity (measured at 1 kHz) versus the level of the addition of PYN for the whole series of the samples studied in this work. As seen from this graph two different trends can mainly be realized. Initially, the magnitudes of the relative permittivity increased for the samples doped up to 2.5 mol% PYN. However, beyond this level, it declined to even lower values than that of the pure PZT compound.

Fig. 4 also demonstrates the results of the r.t. dielectric loss variation measured at 1 kHz versus PYN concentration. As is clear from this graph there is a nearly two times increase in the magnitudes of the dielectric loss upon doping PZT samples with 2.5 mol% of PYN. However, doping PZT samples above this level did not give rise to an appreciable change of dielectric loss compared to the initial observed trend. The variation of the electrical resistivity versus PYN level is also shown in Fig. 5. For the samples doped up to 2.5 mol% PYN the magnitudes of the electrical resistivities of the samples were seen to decline. However, a rising trend was observed for the samples doped above this level. Further, Figs 6 and 7 display separately the variation of d_{33} and g_{33} parameters versus the level of PYN respectively. Increasing the level of PYN to 2.5 mol% caused an increase in the magnitudes of the d_{33} parameter. Further increase of the level of PYN caused a drastic decrease of this parameter. The addition of PYN was also seen to decrease g_{33} parameter (Fig. 7).

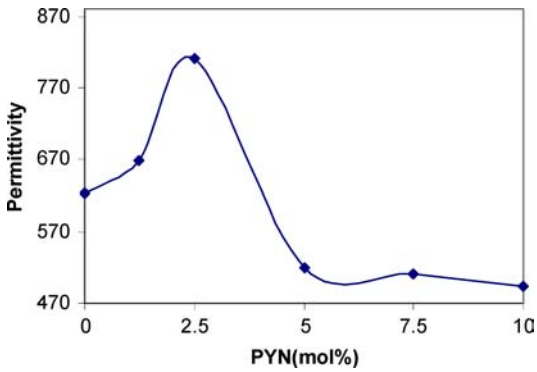

Figure 3 Variation of the room temperature relative permittivity versus $Pb(Y_{0.5}Nb_{0.5})O_3$ (PYN) concentration.

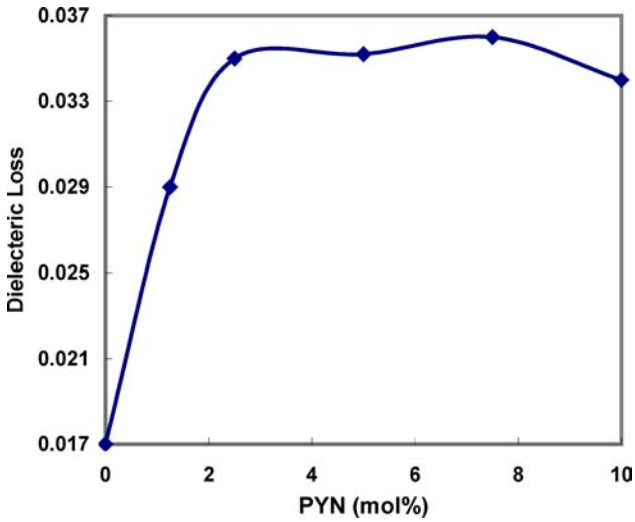

Figure 4 Variation of dielectric loss versus $Pb(Y_{0.5}Nb_{0.5})O_3$ (PYN) concentration.

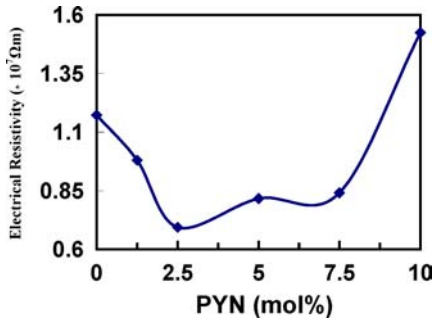

Figure 5 Variation of electrical resistivity versus $Pb(Y_{0.5}Nb_{0.5})O_3$ (PYN) concentration.

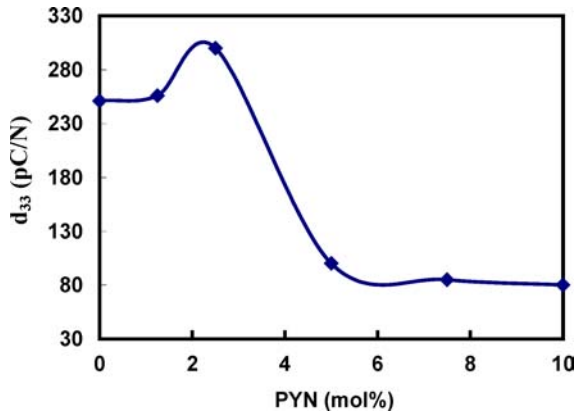

Figure 6 Variation of d_{33} parameter versus $Pb(Y_{0.5}Nb_{0.5})O_3$ (PYN) concentration.

3.4. Microstructural results

Microstructural studies carried out by SEM revealed that doping PZT samples with PYN give rise to grain size reduction of the samples. The average measured sizes of the grain sizes of the samples with 0.0, 1.25, 2.5, 5, 7.5 and 10 mol% PYN were 15.2, 11.3, 3.3, 1.6, 1.3 and 1.2 (μm) respectively. As can be realized from these average values, the observed size reduction was much more pronounced

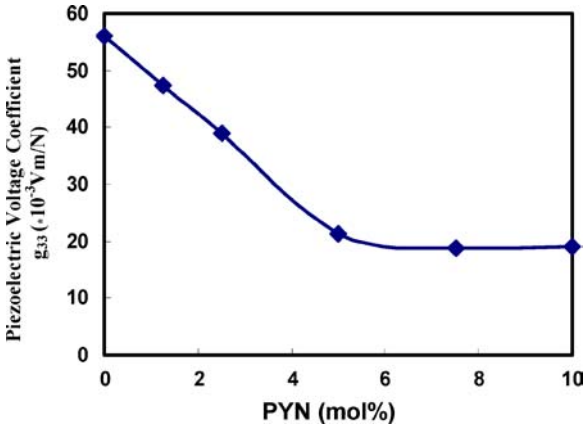

Figure 7 Variation of g_{33} parameter versus $Pb(Y_{0.5}Nb_{0.5})O_3$ (PYN) concentration.

for the samples doped with more than 2.5 mol% PYN. Figs 8 and 9 demonstrate the microstructures of the pure PZT and that of the sample doped with 10 mol% PYN. The formation of the extra second phase for the samples doped above 2.5 mol% PYN was also confirmed by the EDS analysis in close agreement with XRD data. Fig. 10a and b, shows the typical EDS-SEM analysis of the main PZT and extra phase observed for the samples doped with 10 mol% PYN.

4. Discussions

Based on XRD results obtained it can be assumed that there is a limited solid solubility of PYN in PZT compound. The limited solid solubility of Y^{+} [15] and Gd^{3+}[17] in PZT was already reported. Further, as shown in Table I the substitution of PYN up to 2.5 mol% gave rise to the reduction of the volume of unit cell. These can be understood based on the knowledge that Y^{3+} ionic radius (0.99Å) size is smaller than that of the Pb^{2+} (1.49 Å) and much bigger than that of Zr^{4+} (0.72Å) or Ti^{4+} (0.61 Å). The limited solid solubility of Y^{3+} in PZT is thought to be related to the rather big difference of the ionic sizes of Y^{3+} and Pb^{2+}. Nb^{5+} (0.64 Å) can be also expected to be mainly substituted for the Zr^{4+} or Ti^{4+} cations. The observed structural shift from tetragonal to rhombohedral phase for the samples doped with more than 2.5 mol% PYN can be justified by considering the smaller ionic radius of Nb^{5+}compared to that of the Zr^{4+} and the stronger Nb—O bond. In this respect it can be expected that O^{2-} will shift towards Nb^{5+} cation and Pb^{2+} will also depart from its normal position towards Nb^{5+} due to the restriction induced by Pb-O bond. Hence, one can expect that the perovskite structure will then contract giving rise to a gradual change of the symmetry axis from <001> direction to <111>. For the samples containing higher levels of Nb^{5+} the deformation becomes larger leading to crystal structure change from that of tetragonal to rhombohedral.

A decreasing trend was noticed for the electrical resistivities of the samples doped up to 7.5 mol% PYN. However, the rate of the decline was much more pronounced for the samples doped up to 2.5 mol% PYN. The observed rise in the conductivity of these samples is possibly due to the substitution of donor cations such as: Nb^{5+} for Zr^{4+} and Y^{3+} for Pb^{2+} in PZT lattice. Further, the observed rather sharp rise of conductivities for the samples doped up to 2.5 mol%PYN suggests a low level of Pb loss in these samples. Since the donor additives normally are compensated by acceptor sites formed in PZT by lead vacancies [1, 18]. Further, one should also consider the rising increase of Pb vacancies ($V_{pb''}$) with increasing level of the substitutions of Nb^{5+} for Zr^{4+} and Y^{3+} for Pb^{2+} and their corresponding increased donor compensating effect by considering that:

$$2Nb^{5+}_{Zr^{4+}} = 2Nb_{Zr^{*}} + V_{Pb} \quad (1)$$

$$2Y^{3+}_{Pb^{2+}} = 2Y_{Pb^{*}} + V_{Pb} \quad (2)$$

This is possibly why the trend of the decline of the resistivity becomes less pronounced for the samples doped between 2.5 to 7.5 mol% PYN. The observed sharp rise of the resistivity in case of the sample doped with 10 mol% PYN could be possibly partly due to such an effect. However, it should be mentioned that microstructural features such as grain sizes also play an important role in the control of the electrical resistivities of these samples. It is well known [4] that in polycrystalline electroceramics, the lower the grain size the higher will be the electrical resistivities of the samples since the grain boundaries act as a major source of electron scattering centers. As mentioned before the substitution of PYN in PZT samples studied in this work gave rise to the decrease of the average grain sizes of the samples. The decrease of the average grain size was comparatively much higher in case of the samples doped with 10 mol% PYN (Fig. 9). It should be mentioned that the addition of Nb^{5+} to PZT is seen to inhibit the grain growth [19].

Atkin [8], reported that sintering kinetics of the undoped PZT can be described by lattice diffusion of vacancies from pores to grain boundaries (Coble's model), and that Nb doping reduces the diffusion coefficient; the vacancies as created by this doping are supposed to be bound to the impurity ion (Nb), so that they inhibit the mass transport. It should be also added that apart from Nb effect, pores, phase inclusions and solid solution impurities are also known [20] to inhibit the grain growth as well.

The observed sharp rise of the resistivity of this sample could be also partly influenced by the observed grain size reduction. Apart from the above two mentioned factors controlling the conductivity of these samples, one should also consider the contribution of the electrical resistivity of the extra phase to the overall electrical

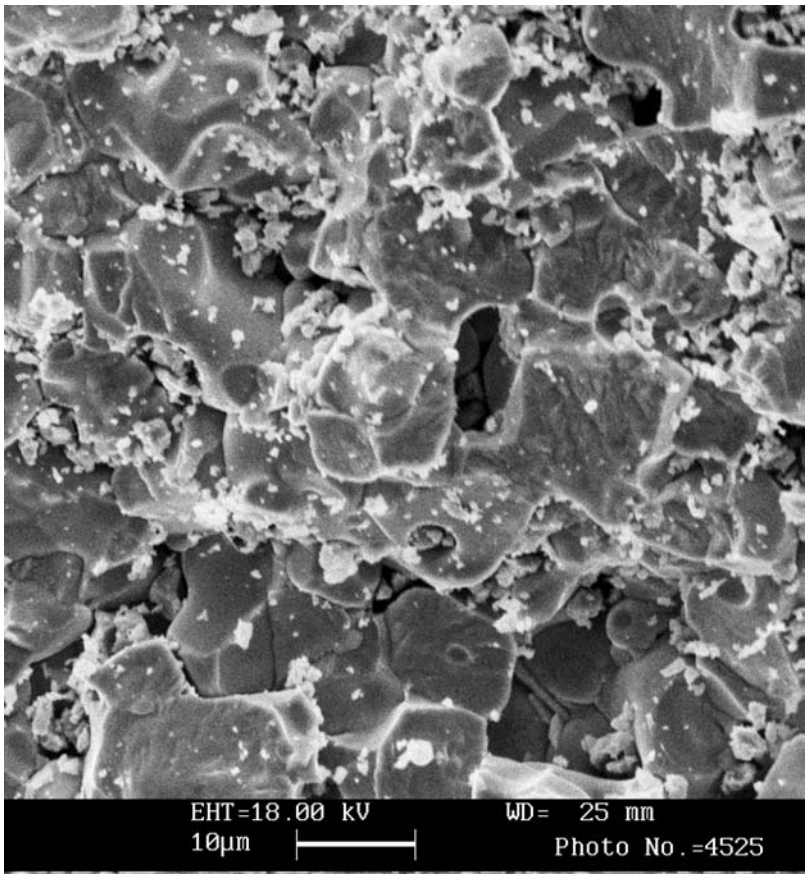

Figure 8 SEM micrograph of the undoped PZT sample.

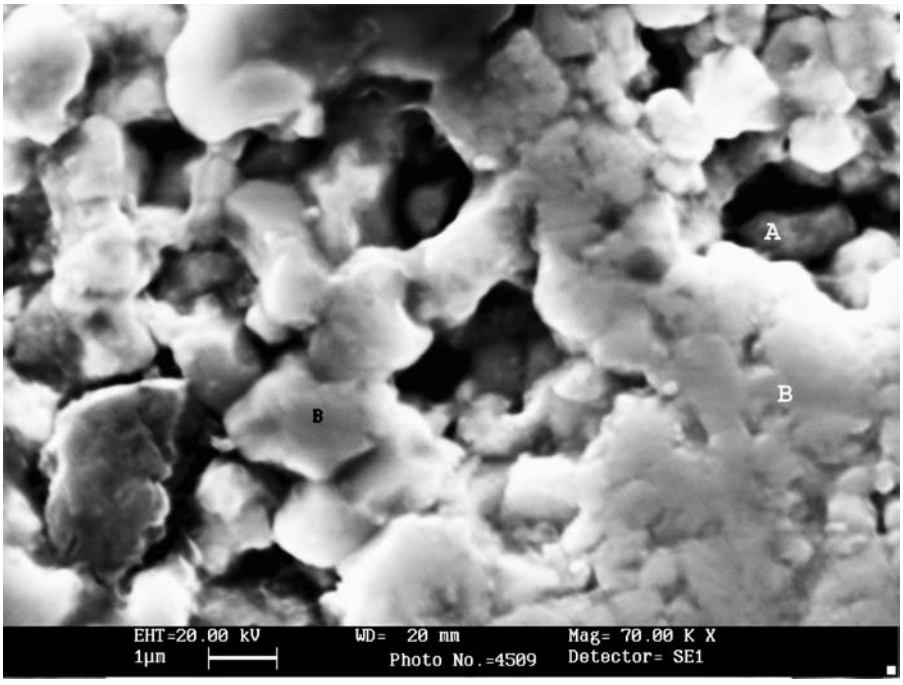

Figure 9 SEM micrograph of the PZT sample doped with 10 mol% $Pb(Y_{0.5}Nb_{0.5})O_3$ (PYN). The EDS analysis of the points A and B is presented in Fig. 10(a) and (b).

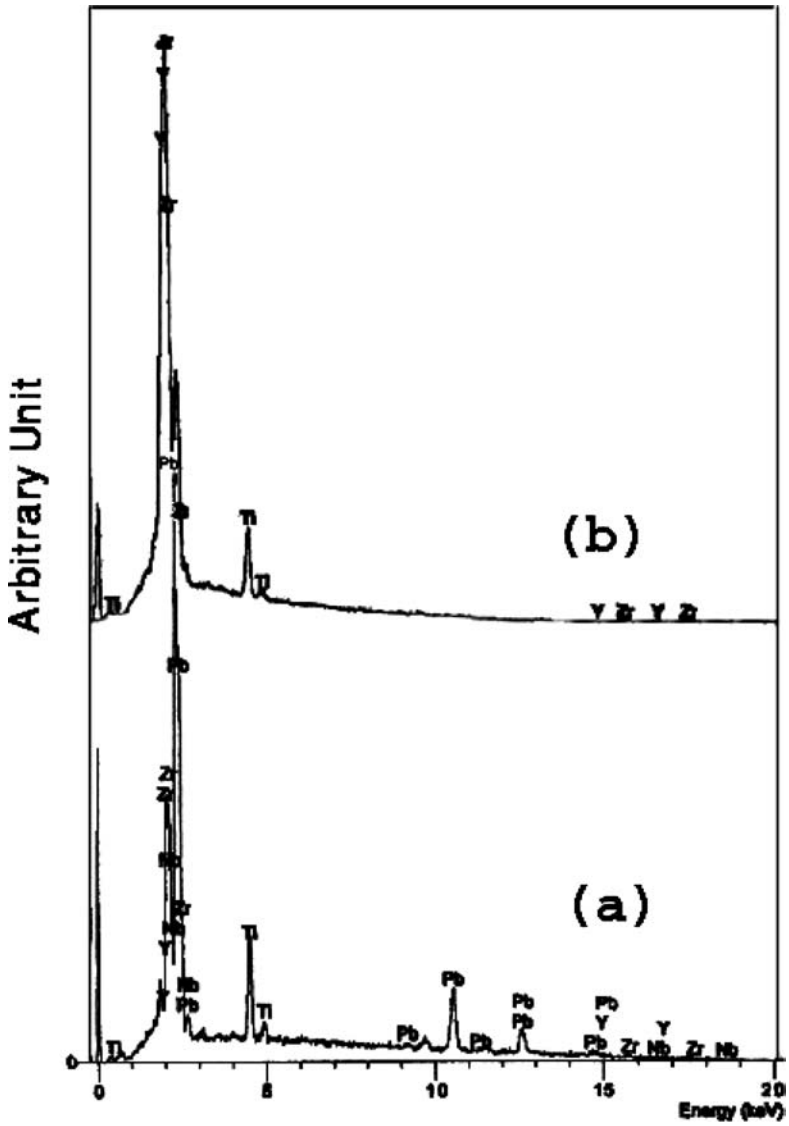

Figure 10 SEM-EDS analysis of the PYNZT main phase (a) (point B in Fig. 9) as well as that of the observed second phase (b) (Point A in Fig. 9).

conductivity of the samples containing this extra phase.

For the samples doped up to 2.5 mol% PYN, a rise in the magnitudes of the relative permittivity was seen (Fig. 3). The observed rise could also be related to the soft ferroelectric behavior introduced due to donor doping and observed noticeable increase of the sintered densities of these samples. However, ferroelectric P-E measurement will be conclusive in this respect. It should be mentioned that donor doping in PZT would be expected to reduce the concentration of oxygen vacancies leading to a reduction in the concentration of domain-stabilizing defect pairs and to a lower ageing rates as well. The resulting increase in domain wall mobility causes the increase of permittivity, dielectric losses, elastic compliance, coupling coefficients, and reductions in mechanical Q and coercivities of the PZT samples.

For the samples doped beyond 5 mol% PYN the magnitudes of the relative permittivity were seen to decrease. The formation of inter/intra granular second phase/s can be considered to have an adverse effect on the mobility of the ferroelectric domain walls. Our microstructural investigations carried out by SEM could only reveal the formation of the non ferroelectric PYN phase as an intergranular second phase. The confirmation of the existence of the PYN phase in intragranular form if present in small quantities and volume fraction demand transmission electron microscopy (TEM) examinations which was not done for the samples studied in this work. Further, the declining trend could have also being influenced by the decrease of the sintered densities of the samples. Pereira *et al*. [19] have also shown that the addition of Nb^{5+} more than 1 mol% in PZT give rise to the decrease of maximum relative permittivity and the curie point. The variation of d_{33} parameter versus the level of PYN presented in Fig. 6 is divided into two trends; a rising one up to 2.5 mol% and another sharp declining one for the samples doped above this level. The latter behavior can be possibly related to

the formation of the observed extra phase and the smaller value of electronic polarizability of Y^{3+}compared to that of Pb^{2+}. However, the initial rising trend of d_{33} parameter for the single phase samples is thought to be mainly related to the increase of Pb vacancies.

As mentioned before, a sharp rise in dielectric loss of the samples doped with PYN was observed. The rising trend was noticeably higher for the samples doped up to 2.5 mol% PYN. The sharp decline of electrical resisitivities of these samples can be accounted as one of the reasons for such an abrupt increase of dielectric loss. However, increased domain wall mobility could have also influenced the A.C. dielectric loss trend observed for these samples.

5. Conclusions

The below mentioned conclusions were obtained based on the work carried out.

1. Doping PZT with more than 2.5 mol% PYN caused the formation of some extra non ferroelectric phase containing zirconium and yttrium and titanium oxides.
2. The addition of PYN above 2.5 mol% to PZT compound caused a structural shift from tetragonal to rhombohedral.
3. The addition of 2.5 mol% of $Pb(Y_{0.5}Nb_{0.5})O_3$ to PZT gave rise to the increase of various ferroelectric parameters such as d_{33}, relative perimittivity and sintered densities. The increase of the ferroelectric parameters is thought to be mainly due to the soft ferroelectric behavior induced by the Pb vacancy formation.
4. The formation of the extra phase had a drastic effect on the various dielectric and piezoelectric parameters.
5. The addition of PYN gave rise to the decrease of the grain sizes of the samples compared to that of undoped PZT samples.

Acknowledgments

The authors would like to express their thanks to Iran Electronic Component Industries (IECI), Shiraz, Iran, Mr.Akbari and Mr.Souli from IECI for their kind helps in our electrical measurements. Further, we acknowledge the support of the department of the metallurgy and Materials Engineering of Iran University of Science and Technology (IUST), Tehran, Iran, regarding the research work carried out.

References

1. B. JAFFE, W. R. COOK and H. JAFFE, in "Piezoelectric Ceramics" (Academic Press, New York, 1971) p. 135.
2. D. A. BERLINCOURT, C. C. MOLIK and H. JAFFE, Proceeding of the IRE, (1960) p. 220.
3. B. JAFFE, R. S. ROTH and S. MARZULLO, *J. Resea. National, Bureau. Sta.* **55** (1955) 240.
4. A. J. MOULSON and J. M. HERBERT, in "Electroceramics, Materials, Properties and Applications" (Chapman and Hall, London, 1990).
5. K. KAKEGAWA and J. MOHRI, *J. Solid. State Commun.* **24** (1977) 769.
6. S. VENKATARAMANI and J. V. BIGGERS, *J. Am. Ceram. Soc. Bull.* **59** (1980) 462.
7. B. V. HIREMATH, I. KINGON and V. BIGGERS, *J. Am. Ceram. Soc.* **66** (1983).
8. R. B. ATKIN and R. M. FULRATH, *ibid.* **54** (1971) 265.
9. S. K. SAHA and D. C. AGRAWAL, *Am. Ceram. Soc. Bull.* **71** (1992) 1424.
10. R. GERSON and H. JAFFE, *J. Phys. Chem. Solids.* **24** (1963) 979.
11. S. J. YOON, H. J. KIM, H. J. JUNG and C. Y. PARK, *Ferroelectrics* **145** (1993) 1.
12. C. LI, M. LIU, Y. ZENG and D. YU, *Sensors and Actuators A* **58** (1997) 245.
13. R. P. TADON and V. SINGH, *J. Mat. Sci. Lett.* **13** (1994) 810.
14. R. P. TADON, V. SINGH and N. N. SWAMI, *Mat. Lett.* **20** (1994) 165.
15. A. BEITOLLAHI and C. H. KHEZRI, *J. Mat. Sci: Mat. Elect.* **12** (2001) 707.
16. P. ARI-GUR and L. BENGUIGUI, *Solid. State. Commun.* **15** (1974) 1077.
17. H. D. SHARMA, A. K. TRIPATHI, V. CHARIAR, T. C. GOEL and P. K. C. PILLAI, *Mat. Sci. Eng.* **25** (1994) 29.
18. R. GERSON and H. JAFFE, *J. Phys. Chem. Solids.* **24** (1963) 979.
19. M. PEREIRA, A. G. PEIXOTO and M. J. M. GOMES, *J. Euro. Ceram. Soc.* **21** (2001) 1353.
20. M. N. RAHAMAN, in "Ceramic Processing and Sintering" (Marcel Dekker, New york, 1995) p. 476

Received 11 April
and accepted 22 August 2005